ELSEVIER

Inorganica Chimica Acta 278 (1998) 217–222

Inorganica Chimica Acta

The 1,8-bis(2′-pyridyl)-3,6-dithiaoctane complex of nickel(II): X-ray crystal structure and borohydride adduct formation

Vitaly V. Pavlishchuk [a,1], Sergey V. Kolotilov [a], Ekkehard Sinn [b], Michael J. Prushan [c], Anthony W. Addison [c,*]

[a] *L.V. Pisarzhevskii Institute of Physical Chemistry of the National Academy of Sciences of the Ukraine, Prospekt Nauki 31, 252039 Kiev, Ukraine*
[b] *School of Chemistry, The University of Hull, Hull HU6 7RX, UK*
[c] *Department of Chemistry, Drexel University, Philadelphia, PA 19104, USA*

Received 15 May 1997; received in revised form 22 July 1997; accepted 18 December 1997

Abstract

The quadridentate dipyridyl-dithioether ligand 1,8-bis(2′-pyridyl)-3,6-dithiaoctane (Pdto) forms a pseudooctahedral complex with nickel(II). Blue $[Ni(Pdto)(OH_2)_2](ClO_4)_2$ crystallizes in the space group $P2_1/c$, with $a = 11.677(5)$, $b = 13.255(2)$, $c = 15.804(4)$ Å, $\beta = 107.45(3)°$ and $Z = 4$. The ligand is folded about the Ni(II) ion so that the water ligands are *cis* within an O_2S_2 plane and the pyridines mutually *trans*. Reduction by sodium amalgam yields a nickel(I) complex with an axial EPR spectrum, whereas borohydride reduction is very slow. Indeed, the pink adduct $[Ni(Pdto)(BH_4)]^+$ has substantial stability in solution. © 1998 Elsevier Science S.A. All rights reserved.

Keywords: Crystal structures; Nickel complexes; Pyridyl-thioether ligand complexes; ESR; Voltammetry; Borohydride adduct

---

1. Introduction

The identification of nickel in a sulfur-donor environment in the active sites of a number of redox proteins, such as the CO-dehydrogenases, has drawn renewed attention to the structure and reactivity of nickel complexes. In particular those with thiolate and/or thioether ligands, which have been advanced as simple models for these active sites [1–13]. In addition, the likely role of nickel(I) as an intermediate in biological processes serves as a justification for examining the Ni(I) states of relevant complexes. Recently, a number of Ni(II) complexes have been isolated with thioether-containing pyridine ligands, including 1,6-bis(2′-pyridyl)-2,5-dithiahexane (**L1**), 1,9-bis(2′-pyridyl)-2,5,8-trithianonane (**L2**) [14], 2-(2′-pyridyl)ethanethiol, and 2-(methylthiomethyl)pyridine [15,16]. A logical addition to this group of complexes is the Ni(II) complex with the ligand 1,8-bis(2′-pyridyl)-3,6-dithiaoctane (Pdto, Fig. 1) [17–19]. We present here chemistry of the Ni-Pdto system and comment on its relationship to some other similar nickel(II) compounds.

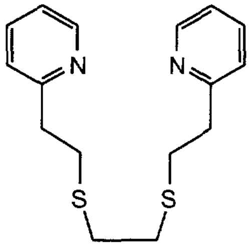

Fig. 1. The ligand Pdto.

2. Experimental

Reagents (Aldrich and ReaChim) were generally used as received. Electronic spectra were recorded on Specord M40 and Perkin-Elmer Lambda-3 spectrophotometers. Electrochemical measurements were carried out on a Preciziyni Pristroyi PI-50 potentiostat, using a three-electrode configuration, incorporating Pt working, auxiliary electrodes and an SCE as reference. The supporting electrolyte was anhydrous sodium perchlorate (the $E_{1/2}$'s are thus approximate values); solutions were deoxygenated by bubbling with argon. EPR spectra were obtained on a Varian E-12 instrument, and calibrated near $g = 2$ with diphenylpicrylhydrazyl.

---

* Corresponding author. Tel.: +1-215-895 2646; fax: +1-215-895 1265; e-mail: addisona@duvm.ocs.drexel.edu

[1] Also corresponding author. E-mail: pavlisvv@phyche.freenet.kiev.ua

PII S0020-1693(98)00030-9

2.1. $Ni(Pdto)(ClO_4)_2 \cdot 2H_2O$

$Ni(ClO_4)_2 \cdot 6H_2O$ (1.83 g, 5.0 mmol) in ethanol (15 ml) was added to an ethanol solution (15 ml) of Pdto (1.52 g, 5.0 mmol) at room temperature. Bright blue crystals formed from the dark blue solution after a few hours, and following evaporative concentration, the product was filtered off and recrystallized from ethanol. Yield: 85%. *Anal.* Calc. for $C_{16}H_{24}O_{10}N_2S_2Cl_2$: C, 32.1; H, 4.04; N, 4.68. Found: C, 32.35; H, 3.91; N, 4.65%. Magnetic moment: 2.6 BM. The complex does not appear to be mechanically sensitive, though perchlorates should be treated with due caution.

2.2. X-ray data collection

All measurements were made as previously described [20] using a Rigaku AFC6S diffractometer with graphite-monochromated Mo Kα radiation, on a blue lozenge of $Ni(Pdto)(ClO_4)_2 \cdot 2H_2O$ with the approximate dimensions of $0.75 \times 0.35 \times 0.30$ mm, mounted on a glass fibre. Diffraction intensities were collected at 295 K by using the ω-2θ scan technique to a maximum 2θ value of 54.1°. Scans of $1.68 + 0.30 \tan(\theta^\circ)$ were made at a rate of 8.0 deg. min^{-1} (in ω). Stationary background counts were recorded on each side of the reflections. Based on the systematic absences ($h0l$, $h+l=2n+1$; $0k0$, $k=2n+1$), a statistical analysis of intensity distribution as well as the successful solution and refinement of the structure, the space group was determined to be $P2_1/n$. Cell constants and the orientation matrix for data collection, obtained from a least-squares refinement using the setting angles of 25 carefully centered reflections in the range $18.2° < 2\theta < 27.5°$, corresponded to a monoclinic cell with dimensions: $a = 11.677(5)$, $b = 13.255(2)$, $c = 15.804(4)$ Å and $\beta = 107.45(3)°$. Of the 3930 reflections collected, 3670 were unique ($R_{int} = 0.109$); equivalent reflections were averaged. Of these, 2552 reflections had $F_o^2 > 3\sigma_{F_o^2}$ where $\sigma_{F_o^2}$ was estimated from counting statistics [20,21]. Lorentz-polarization and absorption [22] corrections were applied. The intensities of three standard reflections, measured after every 150 reflections, showed no greater fluctuation than expected from Poisson statistics. The metal and halogen positions were determined from a 3-D Patterson synthesis based on all data. This phased the data sufficiently to locate the other atoms from difference Fourier maps. The non-hydrogen atoms were refined anisotropically. Full matrix least-squares refinement was carried out using the TEXRAY [23] program set, giving unweighted and weighted agreement factors of $R = 0.038$ and $R_w = 0.038$. The standard deviation of an observation of unit weight was 2.66. The weighting scheme was based on counting statistics and included a factor ($p = 0.01$) to downweight the intense reflections. Plots of $\Sigma_w(|F_o| - |F_c|)^2$ versus $|F_o|$, reflection order in data collection, $\sin(\theta/\lambda)$, and various classes of indices showed no unusual trends. Neutral atom scattering factors were taken from Cromer and Waber [24]. Anomalous dispersion effects were included in F_{calc} [25]; the values for $\Delta f'$ and $\Delta f''$ were those of Cromer [26], and the structures were plotted as ORTEP [27] diagrams. Crystal data are given in Table 1 and positional parameters in Table 2, while Table 3 contains selected bond lengths and angles.

Table 1
Crystal data

Empirical formula	$C_{16}H_{24}Cl_2N_2NiO_{10}S_2$
Formula weight	598.10
Space group	$P2_1/n$
Dimensions (mm)	$0.75 \times 0.35 \times 0.30$
a (Å)	11.677(5)
b (Å)	13.255(2)
c (Å)	15.804(4)
V (Å^3)	2334(2)
Z	4
D_{calc} (g cm^{-3})	1.70
μ (Mo Kα, cm^{-1})	12.90

Table 2
Positional parameters and B_{eq} for $[Ni(Pdto)(OH_2)_2](ClO_4)_2$

Atom	x/a	y/b	z/c	B_{eq}
Ni	−0.02925(6)	0.01128(4)	0.24225(4)	1.82(2)
Cl(1)	−0.2955(1)	0.0635(1)	−0.04707(9)	3.11(6)
Cl(2)	−0.3740(1)	0.1283(1)	0.3875(1)	3.52(7)
S(1)	0.1824(1)	0.0393(1)	0.26822(8)	2.55(6)
S(2)	−0.0108(1)	0.0836(1)	0.38536(8)	2.37(5)
O(1)	−0.0589(3)	−0.0706(2)	0.1229(2)	2.7(1)
O(2)	−0.2202(3)	−0.0026(3)	0.2098(2)	2.7(1)
O(11)	−0.3875(4)	0.0485(3)	−0.1273(2)	5.6(2)
O(12)	−0.1924(4)	0.0048(3)	−0.0452(2)	5.6(2)
O(13)	−0.2657(4)	0.1671(3)	−0.0359(3)	6.4(2)
O(14)	−0.3349(4)	0.0315(4)	0.0258(3)	6.0(2)
O(21)	−0.3260(5)	0.0688(3)	0.3333(3)	7.8(3)
O(22)	−0.3678(6)	0.2276(3)	0.3682(4)	9.7(3)
O(23)	−0.4918(6)	0.1079(6)	0.3748(6)	16.1(6)
O(24)	−0.3224(9)	0.1095(6)	0.4716(4)	18.7(6)
N(1)	−0.0005(4)	−0.1304(3)	0.3054(2)	2.2(2)
N(2)	−0.0460(3)	0.1512(3)	0.1766(2)	2.1(2)
C(2)	0.0902(5)	−0.1952(4)	0.3088(3)	2.5(2)
C(3)	0.0979(5)	−0.2862(4)	0.3517(4)	3.5(3)
C(4)	0.0138(6)	−0.3130(4)	0.3931(4)	4.0(3)
C(5)	−0.0776(5)	−0.2476(4)	0.3905(3)	3.0(2)
C(6)	−0.0817(4)	−0.1583(4)	0.3472(3)	2.4(2)
C(7)	0.1813(5)	−0.1681(4)	0.2638(3)	3.3(2)
C(8)	0.2603(5)	−0.0785(4)	0.3046(3)	3.3(2)
C(9)	0.2187(5)	0.1123(4)	0.3700(4)	3.7(3)
C(12)	−0.0855(4)	0.2390(4)	0.2019(3)	2.2(2)
C(13)	−0.0796(5)	0.3276(4)	0.1573(4)	3.0(2)
C(14)	−0.0352(5)	0.3279(4)	0.0858(4)	3.3(3)
C(15)	0.0050(5)	0.2397(4)	0.0608(3)	3.0(2)
C(16)	−0.0012(5)	0.1548(4)	0.1069(3)	2.6(2)
C(17)	−0.1352(5)	0.2396(4)	0.2792(3)	2.6(2)
C(18)	−0.0436(5)	0.2177(4)	0.3692(4)	3.0(3)
C(19)	0.1501(5)	0.0808(5)	0.4316(4)	3.5(3)
H(3)	0.1652	−0.3307	0.3549	3.5
H(4)	0.0207	−0.3777	0.4202	4.9
H(5)	−0.1395	−0.2666	0.4168	3.4
H(6)	−0.1455	−0.1104	0.3446	2.7
H(11)	−0.106	−0.0542	0.0828	3.8
H(12)	−0.0915	−0.1498	0.1244	5

(*continued*)

Table 2 (*continued*)

Atom	x/a	y/b	z/c	B_{eq}
H(13)	−0.1105	0.3885	0.1756	2.5
H(14)	−0.0334	0.3888	0.0541	3
H(15)	0.0389	0.2393	0.0117	2.9
H(16)	0.0297	0.0928	0.0907	2.8
H(21)	−0.2493	0.028	0.2433	3.1
H(22)	−0.2698	0.0108	0.1531	4
H(71)	0.2357	−0.2268	0.2684	3.4
H(72)	0.145	−0.1562	0.2036	2.4
H(81)	0.329	−0.0773	0.2873	3.1
H(82)	0.2836	−0.0814	0.3713	3
H(91)	0.3042	0.1077	0.3972	4.1
H(92)	0.1997	0.1803	0.3532	3.9
H(171)	−0.1755	0.3066	0.282	2.6
H(172)	−0.1998	0.1935	0.2693	2.8
H(181)	−0.0718	0.2407	0.4137	2.5
H(182)	0.030(4)	0.249(4)	0.376(3)	3(1)
H(191)	0.162(4)	0.125(4)	0.479(3)	4(1)
H(192)	0.167(4)	0.013(4)	0.449(3)	4(1)

Table 3

Selected bond lengths (Å) and angles (°) for $[Ni(Pdto)(OH_2)_2](ClO_4)_2$

Distances			
Ni–S(1)	2.409(2)	N(1)–C(2)	1.352(6)
Ni–S(2)	2.406(1)	N(1)–C(6)	1.360(6)
Ni–O(1)	2.112(3)	N(2)–C(12)	1.356(6)
Ni–O(2)	2.141(3)	N(2)–C(16)	1.354(6)
Ni–N(1)	2.106(4)	S(1)–C(9)	1.816(5)
Ni–N(2)	2.105(4)	S(2)–C(19)	1.801(6)
S(1)–C(8)	1.812(5)	S(2)–C(18)	1.820(5)
Angles			
S(1)–Ni–S(2)	88.88(5)	N(1)–Ni–N(2)	175.7(2)
S(1)–Ni–O(1)	96.7(1)	O(2)–Ni–N(2)	91.2(1)
S(1)–Ni–O(2)	174.6(1)	O(2)–Ni–N(1)	92.5(1)
S(1)–Ni–N(1)	92.7(1)	Ni–S(2)–C(19)	99.3(2)
S(1)–Ni–N(2)	83.5(1)	Ni–S(2)–C(18)	107.6(2)
S(2)–Ni–O(1)	171.3(1)	Ni–N(2)–C(16)	115.5(3)
S(2)–Ni–O(2)	93.0(1)	Ni–N(2)–C(12)	126.9(3)
S(2)–Ni–N(1)	87.3(1)	Ni–N(1)–C(2)	126.6(3)
S(2)–Ni–N(2)	94.7(1)	Ni–N(1)–C(6)	116.0(3)
O(1)–Ni–O(2)	82.1(1)	Ni–S(1)–C(8)	108.3(2)
O(1)–Ni–N(1)	85.7(1)	Ni–S(1)–C(9)	100.9(2)
O(1)–Ni–N(2)	92.7(1)		

3. Results and discussion

The complex is slightly soluble in methanol and ethanol and quite so in acetonitrile or butyronitrile, though the violet colour and the electronic spectra of nitrile solutions differ from the blue of the alcohol ones, mainly due to the replacement of the coordinated water molecule by acetonitrile (Table 4). Furthermore, the nickel(II) coordination by Pdto is at equilibrium in MeCN, as evidenced by the complex's departure from Beer's Law at lower concentrations ($K_f \simeq 10^3$). The binding is stronger in PrCN.

3.1. Description of the structure

The complex crystallizes as $[Ni(Pdto)(OH_2)_2](ClO_4)_2$ (Fig. 2), the nickel ion having an irregularly octahedral structure defined by the $N_2S_2O_2$ donor set. In the solid state, the perchlorate ions are connected with the cation by hydrogen bonds through a water molecule ligand. The Ni–S bond lengths (2.409 and 2.406 Å) and the Ni–N bond lengths (2.106 and 2.105 Å) are close to those of the corresponding bonds in similar complexes [14,28,29], the structure being closely related to that of $[Ni(L1)(MeCN)_2]^{2+}$ [14]. The bond angles at Ni are in general close to 90°, though some deviations from 90° are observed for the angles S(1)–Ni–O(1), S(1)–Ni–O(2), S(1)–Ni–N(2), S(2)–Ni–O(1), S(2)–Ni–N(2), O(1)–Ni–O(2), O(1)–Ni–N(1) (see Table 3). The electronic spectrum of the complex and its paramagnetism confirm its octahedral structure under various conditions.

3.2. Reactivity in solution

3.2.1. Reduction to $[Ni(I)Pdto]^+$

When a violet solution of $Ni(Pdto)(ClO_4)_2 \cdot 2H_2O$ in MeCN was added under N_2 to equimolar sodium amalgam, the solution turned yellow within 30–40 s, then ultimately became brown, there being no further color change after 10 min of stirring. At ambient temperature, no EPR was apparent. However, Na(Hg) reduction (1:1) of the complex in butyronitrile gave a similarly brown solution and, at 77 K, its deep orange cryogenic glass exhibited a characteristic axial nickel(I) EPR spectrum, with $g_\perp = 2.081(4)$ and $g_\parallel = 2.275(4)$. This EPR spectrum (Fig. 3) for $[Ni(Pdto)]^+$ is quite similar to those for other nickel(I) species incorporating N/S coordination, including $N_2O_2S_2$ [30–32] with the presence of weak features (e.g., near $g = 2.02$) presumably due to the presence of a minor rhombic component.

3.2.2. [Ni(0)Pdto]

Addition of two equivalents of Na-amalgam to $Ni(Pdto)(ClO_4)_2 \cdot 2H_2O$ in MeCN under N_2, followed by stirring with heating for 25 min, caused the solution's color to change to red–violet, and a black deposit formed on the amalgam surface.

These solutions containing the reduced complexes regain their violet color on standing in the air.

3.2.3. Reaction of $Ni(Pdto)(ClO_4)_2 \cdot 2H_2O$ with $NaBH_4$

Freshly prepared solutions of anhydrous $NaBH_4$ in MeCN were used. Combining equimolar amounts of $Ni(Pdto)(ClO_4)_2 \cdot 2H_2O$ and $NaBH_4$ in MeCN yielded a pink solution, which slowly became blue again on exposure to air. This system is further discussed below.

3.3. Electronic spectra

Visible- and UV-region electronic spectral data are listed in Table 4. In MeOH, the spectrum of $Ni(Pdto)(ClO_4)_2$ displays three bands, at 24000, 15100 (sharp) and 13800 cm^{-1} attributed to the ${}^3A_{2g} \rightarrow {}^3T_{1g}(P)$, ${}^3A_{2g} \rightarrow {}^1E_g$, and ${}^3A_{2g} \rightarrow {}^3T_{1g}(F)$ transitions. The spin-forbidden ${}^3A_{2g} \rightarrow {}^1E_g$

Table 4
Electronic spectra

Compound	Medium	ν (cm^{-1}) [ε (1 mol^{-1} cm^{-1})]
Ni(Pdto)$(OH_2)_2(ClO_4)_2$	MeOH	13800 [2.5]; 15100 [2.2]; 25000 [7.1]
Ni(Pdto)$(OH_2)_2(ClO_4)_2$	EtOH	15600 [4.1]; 25900 [10.2]
Ni(Pdto)$(OH_2)_2(ClO_4)_2$	MeCN [a]	11450 [30.4]; 17600 [19.6]; 34100 [10000]
Ni(Pdto)$(OH_2)_2(ClO_4)_2$	PrCN	11400 [35.4]; 17500 [28.6]; 35200 [16000]
Ni(Pdto)$(OH_2)_2(ClO_4)_2$	DMF	13850 [3.09, (sh)]; 14900 [4.05]; 25100 [16]
Ni$(ClO_4)_2 \cdot x H_2O$	DMF	13550 [3.7]; 14900 [3.9]; 25000 [11.1]
Ni(L1)$(MeOH)_2(ClO_4)_2$ [b]	MeCN	10800 (sh); 11800 [30]; 18000 [20]
Ni(L2)$(OH_2)(ClO_4)_2$ [c]	MeCN	10150 (sh); 11400 [50]; 18350 [30]
[Ni(Pdto)]$^+$	MeCN	19400; 11500; 34500 [9×10^2]
[Ni(Pdto)]$^+$	PrCN	17900; 11700; 31800
After aerial reoxidation:	PrCN	17600; 11500
[Ni(Pdto)]°	MeCN	26000 (sh); 20000 (sh)
After aerial reoxidation:		17700; 11500
Ni(Pdto)(MeCN)$(BH_4)(ClO_4)$	MeCN	18450; 11500
After aerial reoxidation:		17200; 11500
Pdto		38900; 38100; 37200
$[Ni_2(Pdmt)_2]^-$ [d]		26300; 22000; 16300 (sh)

[a] With excess Pdto added.
[b] Data from [14]; $Dq = 1180$, $B = 728$ cm^{-1}.
[c] Data from [14]; $Dq = 1140$, $B = 936$ cm^{-1}.
[d] Data from [4]; Pdmt = pyridine-2,6-bis(methanethiolate).

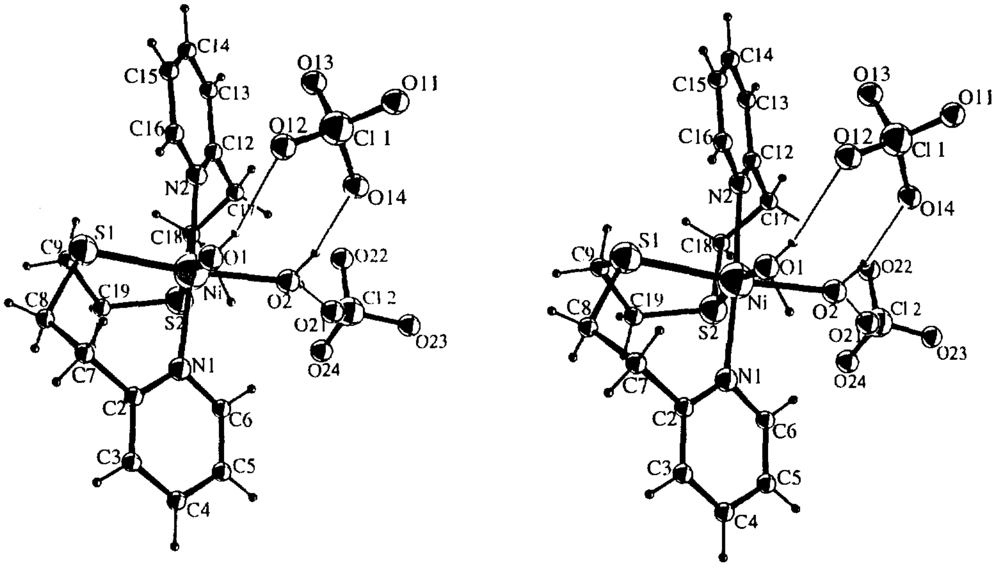

Fig. 2. ORTEP diagram of the formula unit $[Ni(Pdto)(OH_2)_2](ClO_4)_2$ (inverse stereoview).

transition at 15100 cm^{-1} is quite weak. The $^3A_{2g} \rightarrow {}^3T_{1g}(F)$ and $^3A_{2g} \rightarrow {}^3T_{2g}$ bands of $[Ni(Pdto)(MeCN)_2]^{2+}$ in MeCN solution occur at 17600 and 11500 cm^{-1}, and there is a broad charge-transfer band in the UV at 34100 cm^{-1}, shifted from its position in MeOH solution and obscuring the third d–d transition expected for Ni^{2+} [33]. The free ligand has absorption bands at 37000–39000 cm^{-1}, however their shape and position are not very similar to those observed in the complex in this region. The Racah B parameter [33,34] (698 cm^{-1}) for $Ni(Pdto)(MeCN)_2{}^{2+}$ differs significantly from the value for complexes with the 1,6-bis(pyridyl)-2,5-dithiahexane (**L1**), or 1,9-bis(pyridyl)-2,5,8-trithianonane (**L2**) (Table 4) [14]. The value of Dq for $Ni(Pdto)(MeCN)_2{}^{2+}$ (1150 cm^{-1}) lies between that for Ni(**L1**)$(MeOH)_2(ClO_4)_2$ and Ni(**L2**)$(OH_2)(ClO_4)_2 \cdot$MeOH. Lengthening the carbon linkage between the two sulfur donor atoms has an appreciable influence on the spectral properties of the complexes, despite their structural similarity. The data in Table 4 also reveal that in *N*,*N*-dimethylformamide, dissociation of Pdto from Ni(II) is essentially complete at the 10^{-2} M level.

The electronic spectrum of Ni(I)(Pdto)$^+$ produced by Na(Hg) reduction is rather comparable with the 1-electro-

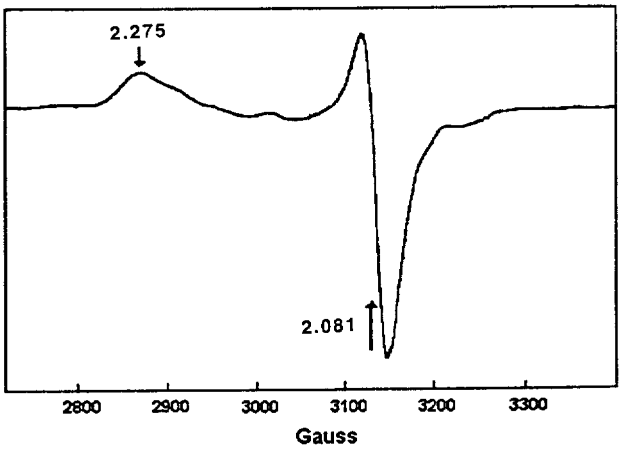

Fig. 3. 77 K X-band cryogenic EPR spectrum of [Ni(Pdto)$(OH_2)_2$]$(ClO_4)_2$ in butyronitrile, reduced with one equivalent of sodium amalgam.

chemical reduction product of the binuclear pyridine-2,6-bis(methanethiolate) nickel complex [4] (Fig. 4, Table 4). The spectrum of this complex is similar to that for a solution of Ni(Pdto)$(MeCN)_2{}^{2+}$ reduced by two sodium equivalents, suggesting that the Na(Hg) reduction is not rapidly stoichiometric. After exposure of the reduced solutions to air, the electronic spectra revert to spectra similar to that of the initial Ni(II) complex. Note that reduction of O_2 leads also to formation of OH^- in solution, which may displace coordinated MeCN. This apparent chemical reversibility of Ni(II)-(Pdto) reduction is confirmed by the electrochemical measurements.

3.4. Reaction with $NaBH_4$

Addition of $NaBH_4$ solution in MeCN to Ni(II)$(Pdto)^{2+}$ in MeCN, under aerobic conditions, causes the violet solution to become pink. The spectrum is again that of a pseudooctahedral nickel(II) system, but the ${}^3A_{2g} \rightarrow {}^3T_{1g}$ (F) band is displaced by 890 cm^{-1}, indicative of the substitution of coordinated MeCN by $BH_4{}^-$. An equilibrium constant was estimated spectrophotometrically using solutions containing a constant total nickel concentration, but $NaBH_4$ in varied ratio. The measurements were carried out at 467 nm, which corresponds to an absorption minimum of Ni(Pdto)$(MeCN)_2{}^{2+}$, ($\varepsilon = 0.07$), where $\varepsilon = 21.5$ for Ni(Pdto)(MeCN)$(BH_4)^+$. This yielded a value of $K = 250 \pm 40$ in MeCN for:

$$Ni(Pdto)(MeCN)_2{}^{2+} + BH_4{}^-$$
$$\rightleftarrows Ni(Pdto)(BH_4)(MeCN)^+ + MeCN$$

Although subsequent further reaction of the $BH_4{}^-$ adduct was relatively slow, in order to estimate K it was necessary to correct this by extrapolating the absorbances to zero time (assuming rapid coordinative equilibration of $BH_4{}^-$ versus MeCN). Indeed, if the procedure was carried out under an argon atmosphere, reduction proceeded gradually, with the ultimate generation of a brown precipitate.

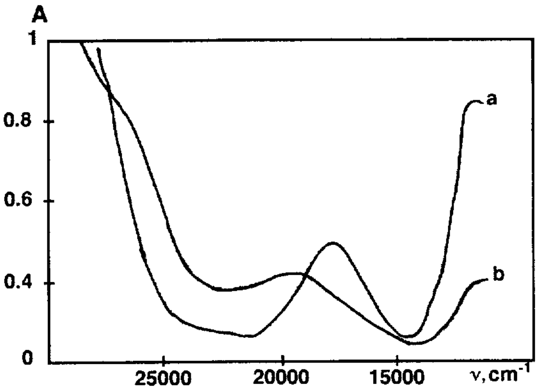

Fig. 4. Optical absorption spectra of (a) [Ni(Pdto)$(OH_2)_2$]$(ClO_4)_2$ in CH_3CN, 0.038 M and (b) 0.016 M solution of [Ni(Pdto)$(OH_2)_2$]$(ClO_4)_2$ in CH_3CN, reduced with one equivalent of sodium amalgam.

3.5. Electrochemistry

The complex displays two redox processes in MeCN, at −0.975 and +0.26 V versus the SCE. The reduction, which we attribute to Ni(I) formation at −0.975 V, is quasi reversible ($\Delta E_p = 150$ mV, $i_a/i_c \approx 1$). This value of $E_{1/2}$ is more negative than those for the nickel complexes with **L1** and **L2**, by 0.19 V and 0.33 V, respectively [14]. Choudhury et al. [35] have pointed out that replacement of N-donors by S-donors raises Ni^{II}/Ni^{I} $E_{1/2}$; this is an interesting parallel to the situation for Cu^{II}/Cu^{I} [36]. The great similarity between the structures of the **L1**- and Pdto-nickel(II) chelates indicates that the difference in $E_{1/2}$'s may lie in the structural details of the lower oxidation states, reflecting the differing lengths of the carbon chains between the sulfur donor atoms. The anodic peak appears at a potential rather too low to be S-oxidation [37,38], so its irreversibility evidences that acyclic ligands with soft donor atoms stabilize nickel(I) better than nickel(III) [14].

Acknowledgements

S.V.K. expresses gratitude to the Soros Fund for supporting his participation in this work (student grant number GSU053074). We thank S.A. Farina for the susceptibility determination. A.W.A. and M.J.P. thank Drexel University for support.

References

[1] D.K. Mills, J.H. Reibenspies, M.I. Darensbourg, Inorg. Chem. 29 (1990) 4364.
[2] W.N. Setzer, C.A. Ogle, G.S. Wilson, R.S. Glass, Inorg. Chem. 22 (1983) 266.
[3] H.-J. Krueger, R.H. Holm, Inorg. Chem. 26 (1987) 3645.
[4] H.-J. Krueger, R.H. Holm, Inorg. Chem. 28 (1989) 1148.
[5] A.T. Kowal, I.C. Zambrano, I. Moura, J.J.G. Moura, J. LeGall, M.K. Johnson, Inorg. Chem. 27 (1988) 1162.
[6] S.G. Rosenfield, M.L.I. Wong, D.W. Stephan, P.K. Mascharak, Inorg. Chem. 26 (1987) 4119.

[7] S.G. Rosenfield, W.H. Armstrong, P.K. Mascharak, Inorg. Chem. 25 (1986) 3014.
[8] S.G. Rosenfield, H.P. Berends, L. Gelmini, D.W. Stephan, P.K. Mascharak, Inorg. Chem. 26 (1987) 2792.
[9] P. Stavropoulos, M. Carrie, M.C. Muetterties, R.H. Holm, J. Am. Chem. Soc. 112 (1990) 5385.
[10] S.P. Cramer, M.K. Eidsness, W.-H. Pan, T.A. Morton, S.W. Ragsdale, D.W. DerVartanian, L.G. Ljungdahl, R.A. Scott, Inorg. Chem. 26 (1987) 2477.
[11] M. Kumar, R.O. Day, G.J. Colpas, M.J. Maroney, J. Am. Chem. Soc. 111 (1989) 5976.
[12] N.R. Bastian, G. Diekert, E.C. Niederhoffer, Boon-Keng Teo, C.T. Walsh, W.H. Orme-Johnson, J. Am. Chem. Soc. 110 (1988) 5581.
[13] M. Kumar, G.L. Colpas, R.O. Day, M.J. Maroney, J. Am. Chem. Soc. 111 (1989) 8323.
[14] B. Adhikary, S. Liu, R. Lucas, Inorg. Chem. 32 (1993) 5957.
[15] J.W. Wrathal, D.H. Busch, Inorg Chem. 2 (1963) 1182.
[16] P.S.K. Chia, S.E. Livingstone, T.N. Locker, Aust. J. Chem. 20 (1967) 239.
[17] H.A. Goodwin, F. Lions, J. Am. Chem. Soc. 82 (1960) 5013.
[18] G.R. Brubaker, J.N. Brown, M.K. Yoo, R.A. Kinsey, T.M. Kutchan, E.A. Mottel, Inorg. Chem. 18 (1979) 299.
[19] S.E. Livingstone, J.D. Nolan, Aust. J. Chem. 23 (1970) 1553.
[20] D.P. Freyberg, G.M. Mockler, E. Sinn, J. Chem. Soc., Dalton Trans. (1976) 447.
[21] P.W.P. Corfield, R.J. Doedens, J.A. Ibers, Inorg. Chem. 6 (1967) 197.
[22] N. Walker, D. Stuart, Acta. Crystallogr., Sect. A 39 (1983) 158.
[23] TEXSAN-TEXRAY, structure analysis package, Molecular Structure Corporation, 1985.
[24] International Tables for X-ray Crystallography, Vol. IV, Kynoch, Birmingham, England, 1974, Table 2.2A.
[25] J.A. Ibers, W.C. Hamilton, Acta Crystallogr. 17 (1974) 781.
[26] International Tables for X-ray Crystallography, Vol. IV, Kynoch, Birmingham, England, 1974, Table 2.3.1.
[27] C.K. Johnson, ORTEP II, Report ORNL-5138, Oak Ridge National Laboratory, Oak Ridge, TN, 1976.
[28] S. Chandrasekhar, A. McAuley, Inorg. Chem. 31 (1992) 480.
[29] A. McAuley, S. Subramanian, Inorg. Chem. 29 (1990) 2830.
[30] M. Zimmer, G. Schulte, X.-L. Luo, R.H. Crabtree, Angew. Chem., Int. Ed. Engl. 30 (1991) 2.
[31] P.J. Farmer, J.H. Reibenspies, P.A. Lindahl, M.Y. Darensbourg, J. Am. Chem. Soc. 15 (1993) 4665.
[32] P. Ge, C.G. Riordan, G.P.A. Yap, A.L. Rheingold, Inorg. Chem. 35 (1996) 5408.
[33] A.B.P. Lever, Inorganic Electronic Spectroscopy, Elsevier, New York, 1984, 2nd edn., p. 507.
[34] S.R. Cooper, S.C. Rawle, J.A. Hartman, Inorg. Chem. 27 (1988) 1209.
[35] S.S. Choudhury, D. Ray, A. Chakravorty, Inorg. Chem. 30 (1991) 4354.
[36] A.W. Addison, Inorg. Chim. Acta 162 (1989) 217.
[37] T.J. Marks, J.R. Kolb, Chem. Rev. 77 (1977) 263.
[38] K. Wieghardt, H.-J. Kuppers, J. Weiss, Inorg. Chem. 24 (1985) 3067.